Soft-phonon instability in zincblende HgSe and HgTe under moderate pressure: *Ab initio* pseudopotential calculations

S. Radescu and A. Mujica
Departamento de Física Fundamental II, MALTA Consolíder Team, and Instituto de Materiales y Nanotecnología, Universidad de La Laguna, La Laguna 38205, Tenerife, Spain

R. J. Needs
Cavendish Laboratory, University of Cambridge, 19 J.J. Thomson Avenue, Cambridge CB3 0HE, United Kingdom
(Received 9 July 2009; revised manuscript received 28 September 2009; published 23 October 2009)

The mercury chalcogenides HgSe and HgTe show peculiar behavior under moderate compression such as the unusual observation of a "hidden" transition from their ambient-pressure zincblende phase to an orthorhombic metastable phase with space group $C222_1$. We present here the results of an *ab initio* pseudopotential study within the framework of the density-functional theory of the stability of the low-pressure zincblende phases of HgSe and HgTe and the transition to the $C222_1$ structure. We relate the observation of the $C222_1$ phase to an instability in the transverse-acoustic phonon branches of the zincblende phases of these materials. We have studied in detail the mechanism of the zincblende $\rightarrow C222_1$ transition as well as the structural evolution of the $C222_1$ phase under pressure.

DOI: 10.1103/PhysRevB.80.144110 PACS number(s): 64.60.Ej, 71.15.Nc, 62.50.−p

I. INTRODUCTION

Under ambient conditions, the mercury chalcogenides HgSe and HgTe crystallize in the zincblende structure. These phases are zero-gap semiconductors, in contrast to the semiconducting low-pressure phases of the zinc and cadmium chalcogenides which together with the mercury chalcogenides form the II-VI family of octet binary compounds. Under applied pressure, HgSe and HgTe exhibit the same sequence of phase transitions.[1] Their ambient zincblende phases transform into semiconducting phases with cinnabar-like structures at pressures around 1 GPa,[1–4] which on further compression transform in turn into the NaCl-type structure[5,6] and then at even higher pressures into the same orthorhombic distortion of the NaCl structure as observed in ZnTe-III (Refs. 7 and 8) and several other members of the binary II-VI and III-V families, the so-called Cmcm phase (after its space group).[1,9]

Except for the existence of a stable cinnabar phase, such a sequence of transitions is not unlike those exhibited by other compounds in the same family. An unusual and interesting feature of HgSe and HgTe is, however, the observation of a transition from the zincblende phase to an orthorhombic phase with space group $C222_1$.[10] This $C222_1$ structure is a distortion of zincblende which has, so far, not been observed in any other binary compound. The zincblende $\rightarrow C222_1$ transition occurs at pressures around ~ 2 GPa, at which the sluggish zincblende $\rightarrow$ cinnabar transition has already begun but has not yet been completed. The $C222_1$ phase is therefore a metastable phase, which would not be observed under conditions of thermodynamic equilibrium, as it would be hidden by the transition to the cinnabar structure. The zincblende $\rightarrow C222_1$ transition in HgSe and HgTe is therefore called a "hidden" transition.[10] Experiments find a small pressure interval in which the zincblende, cinnabar, and $C222_1$ phases coexist, $C222_1$ transforming into the cinnabar phase as the pressure is further increased. Single-phase $C222_1$ has not been obtained in the laboratory.[10]

Although first-principles density-functional theory (DFT) methods have proved valuable for studying high-pressure phases,[9] very few such studies of mercury chalcogenides have been reported so far.[11,12] In this paper we present the results of a first-principles DFT study of the stability of the zincblende structure of HgSe and HgTe and the hidden transition to the $C222_1$ phase which, to the best of our knowledge, has not been considered theoretically before, in these or any other compounds. The region of compressions over which our results pertain is thus that of rather moderate (for today's standards of experimentally accessible compressions) "high" pressure, just slightly above the onset of stability of the first of the high-pressure phases displayed by these compounds, viz. the cinnabar phase. We will leave out of the present discussion the detailed study of the full sequence of pressure-driven transitions undergone by these compounds[13] but, for the sake of completeness, we will show energy-volume plots of their high-pressure cinnabar phases.

The rest of this paper is organized as follows. In Sec. II we give details of our first-principles DFT calculations and in Sec. III we describe the structures considered in our study. We present our results for the structural phases in Sec. IV and finally, in Sec. V, we summarize the conclusions of our study.

II. DESCRIPTION OF THE CALCULATIONS

The pseudopotential plane-wave DFT calculations were performed with the Vienna *ab initio* simulation package (VASP), see Ref. 14 and references therein. We used the projector-augmented wave (PAW) scheme,[15] and the semicore $5d$ and $6s$ electrons of Hg and the outermost s and p electrons of Se and Te were dealt with explicitly in the calculations. Basis sets including plane waves up to a kinetic-energy cutoff of 291.4 eV were used for both HgSe and HgTe in order to achieve highly converged results. Dense Monkhorst-Pack **k**-point grids were used for the Brillouin-

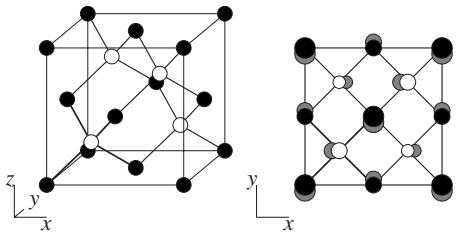

FIG. 1. The zincblende structure, plotted in perspective using a conventional crystallographic cubic cell (left) and in projection onto the *xy* plane (right). The black and white circles represent anion and cation positions, respectively. The gray circles in the projected plot represent the atomic positions in the orthorhombic $C222_1$ structure, in which the atoms are displaced within the *xy* plane with respect to the zincblende structure.

zone integrations. The differences in total energy between phases were converged with respect to the basis set and **k**-point sets employed to within about 1 meV per atom. We used the local-density approximation (LDA) exchange-correlation functional[16] for the results presented in Sec. IV, but we also performed calculations using the generalized gradient approximation (GGA) (Ref. 17) which lead to essentially the same qualitative picture as the LDA results.

A review of the application of DFT-based total-energy methods to the phase stability of semiconductors can be found in Ref. 9. Our theoretical results are for hydrostatic conditions and zero temperature and the small effects of zero-point motion have been neglected. The zincblende structure can be represented using the $C222_1$ description (by adjusting the values of the structural parameters of $C222_1$, see Sec. III) which allows for a very precise comparison between the energetics of these structures. The $C222_1$ and cinnabar structures have free structural parameters which were fully relaxed at each volume through the calculation of the forces on the atoms and the stress tensor. Structural relaxations reduced the anisotropy in the diagonal components of the stress tensor to below ~0.1 GPa and the forces on the atoms to below 0.005 eV/Å. We have found this level of accuracy to be sufficient to account for the structural features of the zincblende phases of HgSe and HgTe under pressure and the transition to the $C222_1$ structure.

III. DESCRIPTION OF THE STRUCTURES

The stable phases of HgSe and HgTe adopt the cubic zincblende structure (hereafter abbreviated zb where appropriate) at ambient conditions. It has space group (SG) $F\bar{4}3m$, No. 216, and $Z=4$ formula units per conventional unit cell, with cations at positions 4(a) (0,0,0) and anions at positions 4(c) (1/4,1/4,1/4). In the zincblende structure each atom has ideal tetrahedral coordination (see Fig. 1).

The orthorhombic $C222_1$ structure is depicted in projection in Fig. 1. The cations occupy positions 4(a) $(x,0,0)$ and the anions occupy positions 4(b) $(0,y,1/4)$ of SG $C222_1$, No. 20, with $Z=4$. The experimental values of the axial ratios and internal parameters of $C222_1$-HgSe (at a volume per formula unit $V=53.2$ Å^3 and pressure $p=2.25$ GPa) and $C222_1$-HgTe (at $V=62.5$ Å^3 and $p=2.55$ GPa) are collected in Table I (Ref. 10), along with our own calculated values (see Sec. IV C). The $C222_1$ structure is a slight distortion of the zincblende structure, which in the $C222_1$ description corresponds to $x=y=0.25$ and $b/a=c/a=1$. The tetrahedral coordination of the zincblende structure is approximately preserved in the $C222_1$ structures observed in HgSe and HgTe.

TABLE I. Experimental (Ref. 10) and theoretical values (calculated in this work) of the structural parameters of the $C222_1$ phases of HgSe and HgTe. These data correspond to the experimental volumes per formula unit reported in Ref. 10 at pressures slightly above 2 GPa for each material.

$C222_1$-HgSe at $V=53.2$ Å^3 ($p\sim2.3$ GPa)				
	b/a	c/a	x(Hg)	y(Se)
Experiment:	0.981	1.009	0.302(1)	0.207(2)
Theory:	0.984	0.998	0.304	0.210
$C222_1$-HgTe at $V=62.5$ Å^3 ($p\sim2.6$ GPa)				
	b/a	c/a	x(Hg)	y(Te)
Experiment:	0.991	1.011	0.315(1)	0.205(2)
Theory:	0.982	0.994	0.301	0.211

Although this work deals mainly with the instability of the zincblende phase and the hidden transition to the $C222_1$ phase, we have also performed calculations for the cinnabar phase for which we show energy-volume curves to give a proper account of the stability limits of the zincblende phase. The trigonal cinnabar-type structure (abbreviated cin) observed at moderately high pressures in HgSe and HgTe and as a zero-pressure stable phase in HgS has SG $P3_121$ No. 152 and $Z=3$, with cations at positions 3(a) $(x_1,0,1/3)$ and anions at positions 3(b) $(x_2,0,5/6)$. Experimentally, x(Hg) $=0.662(1)$, x(Se)$=0.550(1)$, $a=4.120$ Å, and $c/a=2.320$ in HgSe at 46.84 Å^3, 4.0 GPa (Ref. 1), and x(Hg)$=0.641(1)$, x(Te)$=0.562(1)$, $a=4.383$ Å, and $c/a=2.287$ in HgTe at 55.58 Å^3, 3.6 GPa (Ref. 3, see Fig. 2). These values of the internal and cell parameters result in 2+2+2 coordination in cin-HgSe and 4+2 coordination in cin-HgTe under moderately high pressures, and the structure can be viewed as being formed of spirals of atoms along the *c* axis in which cations and anions alternate.[1] The zincblende and cinnabar structures are of course well known and the interested reader may find a fuller description of them in Refs. 1 and 9, and references therein, or in other standard texts.[18,19]

IV. RESULTS AND DISCUSSION

In Figs. 3 and 4 we show the calculated energy-volume curves, $E(V)$, of the zincblende, $C222_1$, and cinnabar phases of (respectively) HgSe and HgTe, obtained using the LDA. [Hereafter all values of extensive quantities are given per formula unit (pfu).] Note the very small energy scale spanned by the axes in these figures. From these plots we can immediately extract conclusions on relative stability using, for example, the standard common tangent construction.[9]

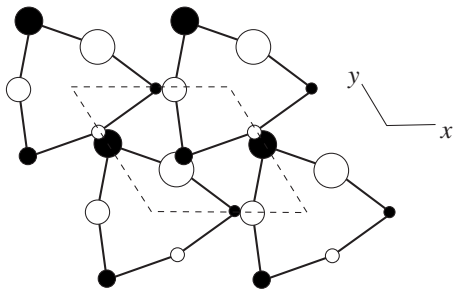

FIG. 2. The cinnabar structure of HgTe at ~3.6 GPa, viewed along its threefold main c axis. (For reference, the outline of the projected unit cell is shown as a dashed line.) The black and white circles represent anion and cation positions, respectively. Atomic planes of like atoms perpendicular to the main axis are uniformly separated by a distance of $c/6$. The differences in height are represented in the projected figure by the different sizes of the atoms. This structure is sometimes described as formed of spirals of atoms along the c axis in which cations and anions alternate. In our drawing the projected spirals are represented by solid lines.

A. The low-pressure zincblende phases: Equilibrium properties and stability

Our calculated zero-pressure equilibrium volume and bulk modulus for zb-HgSe, obtained from fitting the $E(V)$ data to a Murnaghan-type equation of state, are $V_0^{the}=56.23$ Å^3 and $B_0^{the}=57$ GPa, in excellent agreement with the experimental values of $V_0^{exp}=56.30$ Å^3 and $B_0^{exp}=58$ GPa.[20] A similar level of agreement is obtained for zb-HgTe: $V_0^{the}=67.03$ Å^3 and $B_0^{the}=47$ GPa; $V_0^{exp}=67.43$ Å^3 and $B_0^{exp}=48$ GPa.[20]

As mentioned in Sec. II, we have also performed calculations within the PAW scheme but using the GGA for the exchange-correlation functional. Our GGA results for the equilibrium properties of the zincblende phases of HgSe and HgTe are $V_0^{the}=61.87$ Å^3 and $B_0^{the}=42$ GPa for HgSe; and $V_0^{the}=73.96$ Å^3 and $B_0^{the}=34$ GPa for HgTe. These results are in poorer agreement with experiment than the LDA results. In the next sections we present results obtained within the LDA, but we stress that aside from the quantitative discrepancies in the values of the zero-pressure equilibrium properties, the qualitative aspects of our study are quite similar in the LDA and the GGA.

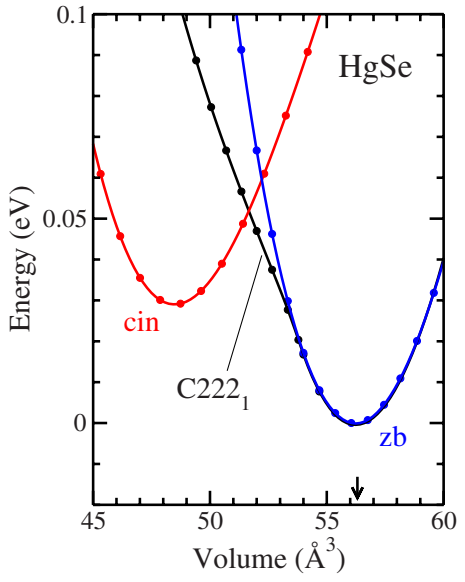

FIG. 3. (Color online) Calculated energy-volume curves for the zincblende, cinnabar, and C222$_1$ phases of HgSe, obtained within the LDA. Both magnitudes are given per formula unit. The energy is given with respect to that of the equilibrium volume of the zincblende phase. The experimental equilibrium volume of the zincblende phase is marked by an arrow.

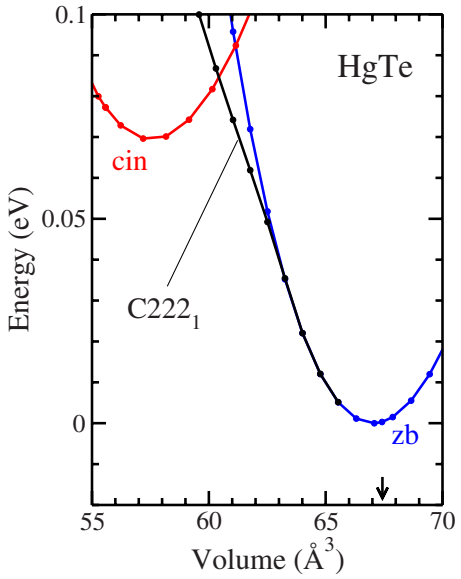

FIG. 4. (Color online) Same as Fig. 3 but for HgTe.

Figures 3 and 4 correctly show the zincblende phase of both HgTe and HgSe to be stable at zero pressure with cinnabar about 30 meV higher in energy and about 14.5% more compressed than zincblende in HgSe (69 meV and 14.2% compression, respectively, in HgTe). The enthalpy differences between the zincblende and cinnabar phases are characteristically smaller in these mercury compounds than in other members of the II–VI and III–V families. In HgS the cinnabar phase is still lower in enthalpy and is the stable phase at zero pressure[1] while in HgO a low-energy cinnabar phase has been experimentally observed as a metastable state under ambient conditions.[21]

Also from Figs. 3 and 4 we see (applying, e.g., the common tangent construction) that under compression the zincblende phases of both HgSe and HgTe become thermodynamically unstable to the cinnabar structure. The calculated zb/cin coexistence pressures are ~0.7 GPa in HgSe and ~1.1 GPa in HgTe, which should be compared with the experimental values of the zb→cin transition pressures of 1.15 GPa in HgSe (Ref. 10) and ~1.3–1.6 GPa in HgTe.[2,22] The calculated structural parameters of the cinnabar phases, given here for the sake of reference, are also in good agreement with those reported in experiments: x(Hg)=0.661, x(Se)=0.569, and $c/a=2.32$ for HgSe at the volume 47.0 Å^3 and x(Hg)=0.642, y(Te)=0.561, and $c/a=2.29$ for HgTe at 55.6 Å^3, cf. the experimental values quoted in Sec. III.

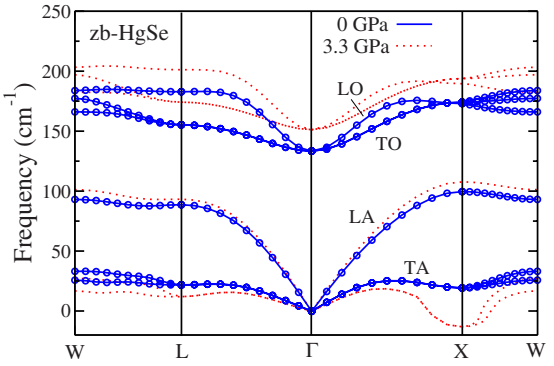

FIG. 5. (Color online) Calculated phonon frequencies of zincblende HgSe plotted along symmetry lines of the Brillouin zone of the zincblende structure. [$\mathbf{k}_\Gamma=0$, $\mathbf{k}_X=(0,0,1)$, $\mathbf{k}_L=(1/2,1/2,1/2)$, $\mathbf{k}_W=(0,1/2,1)$, in units of $2\pi/a$.] Full lines and circles correspond to zero pressure whereas dotted lines correspond to a pressure slightly above 3 GPa.

B. Dynamical instability of the zb phases and the zb→C222$_1$ transition

For both HgSe and HgTe we find that as pressure is applied to the zincblende phase it becomes locally unstable against an orthorhombic distortion leading to the C222$_1$ structure. The onset of the instability of the zincblende phase occurs at ~2–2.3 GPa for HgSe and ~2.4–2.8 GPa for HgTe, that is, slightly above their respective zb/cin coexistence pressure and in excellent agreement with the experimental observations.[10] At the pressures at which the C222$_1$ phase is first observed in HgSe and HgTe, the cinnabar phase is the thermodynamically stable one, but due to the sluggishness of the first-order reconstructive zb→cin transition there is still a significant amount of untransformed low-pressure zincblende phase in a slightly overpressurized, metastable state. Thus, the kinetic barriers to the strongly first-order zb→cin transition allow the zincblende phase to reach a point of dynamical instability where the displacive and essentially barrierless zb→C222$_1$ transition takes place.

The pattern of the C222$_1$ distortion corresponds to a transverse-acoustic (TA) phonon at the Brillouin-zone boundary X point of the zincblende structure [$\mathbf{k}_X=(0,0,1)$ in units of $2\pi/a$], which effectively doubles the unit-cell size with respect to that of zincblende.[23] We have calculated the phonon spectrum of zincblende HgSe and zincblende HgTe at zero pressure and at a compressed volume beyond the onset of the transition to C222$_1$, through the calculation of the force-constants matrix using the method of finite displacements in a $4\times4\times4$ (128 atoms) supercell.[24,25] The calculated frequencies are given in Figs. 5 and 6. As a reference, our calculated frequencies for the zero-pressure transverse-optic (TO) modes at the Γ point are $\omega_{\mathrm{TO}}^{the}(\Gamma)=4.00$ THz in zb-HgSe and $\omega_{\mathrm{TO}}^{the}(\Gamma)=3.45$ THz in zb-HgTe, in excellent agreement with the experimental values $\omega_{\mathrm{TO}}^{exp}(\Gamma)=4.0$ THz (zb-HgSe) and $\omega_{\mathrm{TO}}^{exp}(\Gamma)=3.54$ THz (zb-HgTe).[20,26] The phonon dispersion relations shown in Figs. 5 and 6 exhibit rather low TA branches even at zero pressure. The optic and LA frequencies increase with pressure whereas the low-frequency TA branches soften with pressure and eventually become unstable at the X point which is an extremum for this band.[27] The pressure evolution of the phonon frequencies at Γ and X, obtained using an economical doubled cell which correctly describes the phonon at both points, is given in Figs. 7 and 8.[28]

We note that the onset of the C222$_1$ instability shown in Figs. 7 and 8 [that is, the pressure at which the TA(X) branch gets to zero] is slightly above the onset calculated by full relaxation of the structure, which is around 2–2.5 GPa. At these pressures the calculated frequency of the TA(X) modes

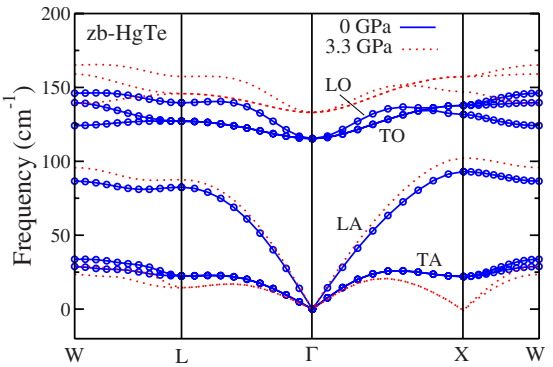

FIG. 6. (Color online) Calculated phonon frequencies of zincblende HgTe plotted along symmetry lines of the Brillouin zone of the zincblende structure. Full lines and circles correspond to zero pressure whereas dotted lines correspond to a pressure slightly above 3 GPa.

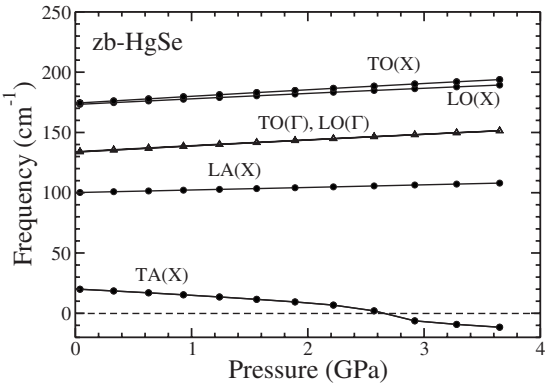

FIG. 7. Evolution with pressure of the calculated phonon frequencies at the X (circles) and Γ (triangles) points of the Brillouin zone of zb-HgSe.

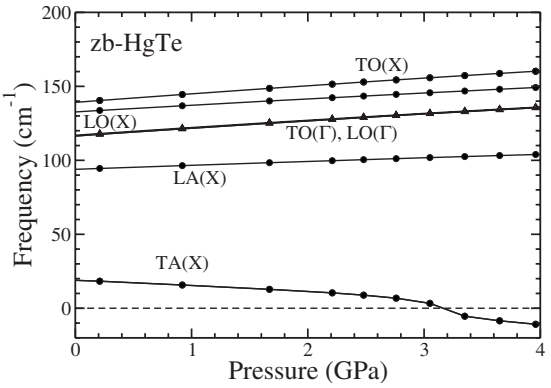

FIG. 8. Same as Fig. 7 but for zb-HgTe.

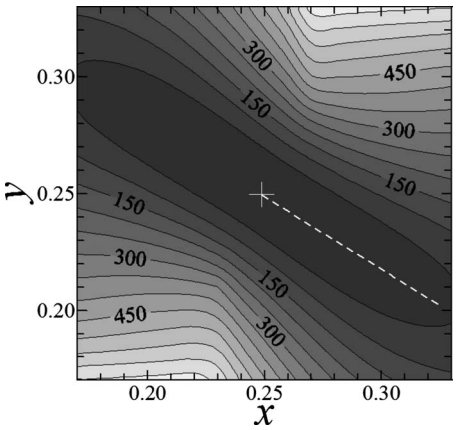

FIG. 9. Contour plot of the energy E of $C222_1$-HgSe as a function of its internal parameters (x,y). This plot is for $V=56.3$ Å^3 ($p\sim 0$ GPa), that is, before the onset of the zb instability. The energy is given in meV and is measured with respect to that of the reference zb structure [which in the plot corresponds to the point (0.25,0.25)]. At each (x,y) point the shape of the cell was fully relaxed. The dashed line indicates the path of minimum-energy change from the zb configuration.

is, however, already very low (around 10 cm^{-1}) and the quasiharmonic approximation may not be adequate here.

C. The $C222_1$ distortion in detail

In Figs. 9 and 10 we show contour plots at two different compressions (below and above the onset of the instability, respectively) of the energy E of the $C222_1$ phase as a function of its two internal parameters (x,y), obtained from full cell-shape relaxation at each fixed value of (x,y). The zincblende structure corresponds to the point (0.25,0.25), which is, by symmetry, a stationary point of $E(x,y)$. Up to moderate compressions (Fig. 9), the zb point is a minimum of the energy of the $C222_1$ phase which means that the zincblende structure is stable against the $C222_1$ distortion. Already at this stage, the energy landscape has the form of a

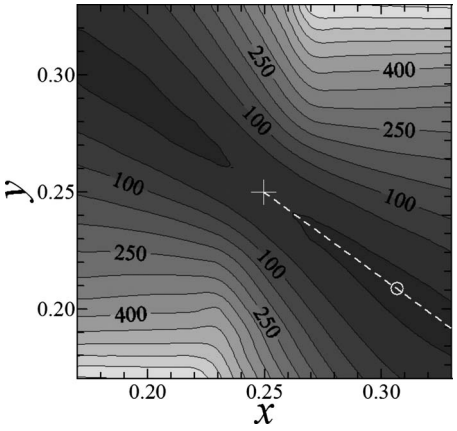

FIG. 10. Same as Fig. 9 but for a volume $V=52.7$ Å^3 ($p\sim 3$ GPa) at which the zb structure is unstable against the $C222_1$ distortion. The calculated minimum-energy $C222_1$ configuration is marked by a circle.

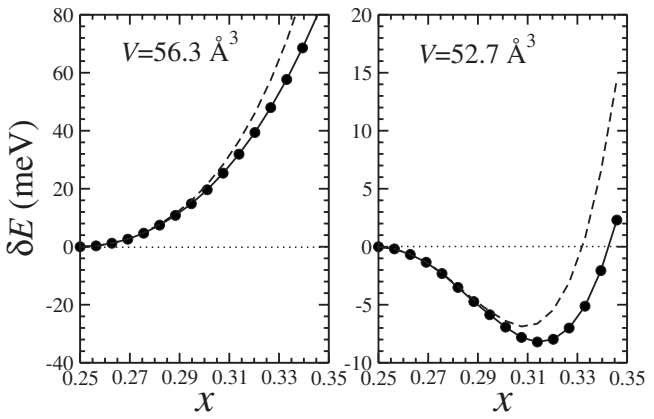

FIG. 11. The change in energy per formula unit along the minimal path shown in Fig. 9 (left panel) and Fig. 10 (right panel). (Note the difference in the energy scales between the panels.) We use the value of the internal parameter x to indicate the position along the path. The solid curve and symbols (which correspond to calculated values) are for full relaxation of the cell shape at fixed volume and each (x,y) point. The dashed curve corresponds to keeping the shape fixed to that of the zb configuration.

rather shallow and narrow valley which defines a path of minimum change in energy along which the energy gain from the zb point is indeed quite small. The direction of this path in (x,y) configuration space corresponds to the calculated eigenvector of the soft TA(X) mode (at this compression not yet unstable).[29] As the compression proceeds (Fig. 10) the zb point at (0.25,0.25) becomes a saddle point, that is, the zincblende structure becomes unstable against a distortion in the direction of the minimum-energy valley, and two new, quite shallow, and symmetrical minima appear along it. These equivalent minima correspond to the distorted $C222_1$ configuration reported in experiments.

In order to show the nature and effect of the instability of the zincblende structure against the $C222_1$ distortion we plot in Fig. 11 the calculated change in energy per formula unit along the deformation path before (left panel) and after (right panel) the instability has set in. Two curves are shown within each of these figures: the dashed ones correspond to fixing the shape of the cell to that of the reference cubic zincblende structure, whereas the solid lines and symbols correspond to full cell-shape relaxation (as in Figs. 9 and 10). From these figures we conclude that the orthorhombic deformation of the cell is a less important mechanism in the energy gain along the deformation path, accounting for just a few meV pfu of the overall gain in the case shown, and that within the range of pressures in which the $C222_1$ phase is observed, the absolute gain in energy associated with the transition into the $C222_1$ structure is in itself rather small even for a well-developed distortion such as that shown in the right panel of Fig. 11.

A small reduction in volume of around 1% has been reported experimentally for the zb$\rightarrow C222_1$ transition in both HgSe and HgTe,[10] which is consistent with the proposed soft-phonon mechanism leading to a weakly first-order transition. As shown in Fig. 11, full relaxation of the $C222_1$ structure results, at the initial stages of the distortion, in a rather shallow minimum which makes it difficult to discrimi-

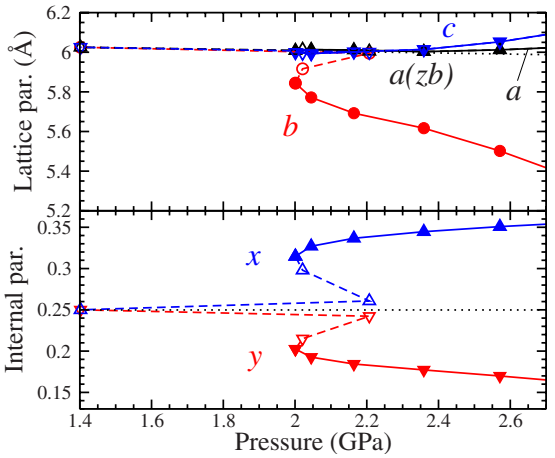

FIG. 12. (Color online) Evolution of the calculated structural parameters of $C222_1$-HgSe with pressure: lattice parameters a, b, and c (upper panel) and internal parameters x and y (lower panel). We have denoted by open symbols and dashed lines those data in the region of instability of the $C222_1$ phase. The dotted lines correspond to values of the parameters for the zincblende phase at the same pressure.

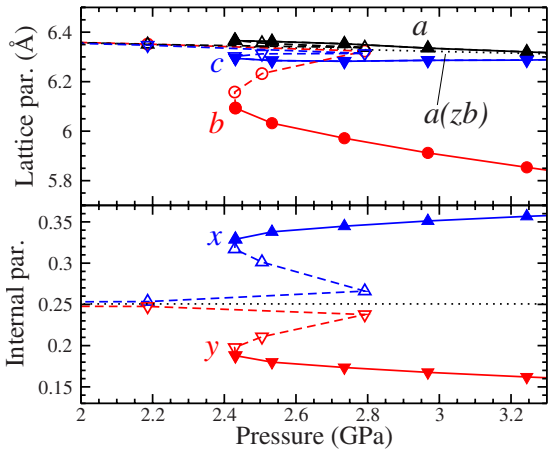

FIG. 13. (Color online) Same as Fig. 12 but for $C222_1$-HgTe.

nate the character of the transition in our calculations. Nonetheless the transition would appear to be indeed first order. Hardly perceptible in Figs. 3 and 4, there is a very subtle downwards concavity in the $E(V)$ curve of the $C222_1$ phases around volumes at which the curve merges with that of the zb phase, indicating a region of instability for $C222_1$ with an associated volume discontinuity. This small region is, however, rather difficult to quantify precisely on account of the very small energy changes involved, and small inaccuracies can somewhat modify its extension. The region of instability also shows up in the pressure evolution of the structural parameters (see below).

For HgSe at the volume 53.2 Å^3 reported in experiments[10] ($p \sim 2.3$ GPa) we find values of the internal parameters and axial ratios x(Hg)=0.304, y(Se)=0.210, b/a=0.984, and c/a=0.998, in excellent agreement with the experimental values reported in Ref. 10, see Table I. A similar level of agreement between the calculated and experimental values of the structural parameters is obtained for HgTe at the volume 62.5 Å^3, $p \sim 2.6$ GPa, for which our calculated values are x(Hg)=0.301, y(Te)=0.211, b/a=0.982, and c/a=0.994.

In Figs. 12 and 13 we show the evolution with pressure of the calculated structural parameters of the $C222_1$ phases of HgSe and HgTe, respectively. In these figures we have denoted the region of instability of the $C222_1$ phases by using open symbols and dashed lines. For comparison, we have also included in these figures data for the zincblende phase (dotted lines). At low pressures the values of both the x and y internal parameters of the $C222_1$ phases tend to 0.25, and the axial ratios b/a and c/a tend to 1, which corresponds to the special case of the zincblende structure (see Sec. III). At these higher volumes/lower pressures the $C222_1$ distortion is thus suppressed. Figures 12 and 13 also show the discontinuity in the structural parameters at the transition. As seen in these figures, the transition to $C222_1$ is accompanied in both materials of a reduction in the value of the b parameter (with respect to the zb value) while the a and c parameters are relatively insensitive to the instability. The $C222_1$ phase appears to be rather compressible along its b axis in the relevant pressure range around 2–3 GPa. Experimentally, the larger change in lattice parameters at the transition was observed for the b parameter, both in HgSe and HgTe, but no pressure evolution of the structural parameters has been reported.[10]

The ideal tetrahedral coordination of the zincblende phase is distorted at the $C222_1$ transition. In $C222_1$ the coordination is 2+2, with one nearest-neighbor (nn) distance larger than in the reference zincblende structure at the same pressure and the other smaller, see Fig. 14, but the *mean* nn distance is larger in $C222_1$ than in zincblende at the same pressure. This may seem surprising because the volume in $C222_1$ is of course smaller than in zincblende at the same pressure. As the compression is increased, the *large* distance increases and the *small* distance decreases.

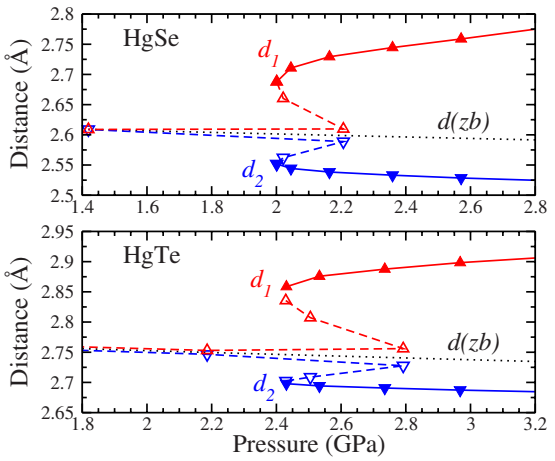

FIG. 14. (Color online) Evolution with pressure of the calculated nearer neighbor distances (d_1 and d_2) of $C222_1$-HgSe (upper panel) and $C222_1$-HgSe (lower panel). Data in the region of instability of $C222_1$ are denoted by open symbols and dashed lines. The nearest-neighbor distance of the zincblende phases, d(zb), is also given (dotted lines), for reference.

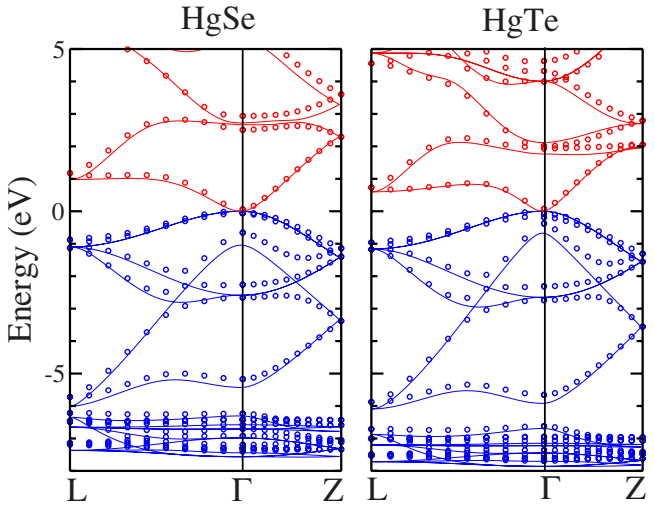

FIG. 15. (Color online) The calculated Kohn-Sham electronic band structure of the $C222_1$ phases of HgSe (left panel) and HgTe (right panel) along two symmetry lines from the Γ point (circles). [$\mathbf{k}_\Gamma=0$, $\mathbf{k}_Z=(0,0,1/2)$, and $\mathbf{k}_L=(1/4,1/4,1/4)$ in units of $(4\pi/a,4\pi/b,4\pi/c)$.] The zero of the energy scale is set at the middle of the small gap at Γ (which is hardly discernible in the scale of the figures). These figures are for volumes of 53.2 $Å^3$ (HgSe) and 62.5 $Å^3$ (HgTe) for which structural data have been reported experimentally (Ref. 10). The calculated band structures of the respective zincblende phases at the same volumes are also given for reference (full lines).

Finally we mention briefly the effect of the $C222_1$ distortion on the band structure. The zincblende phases are zero-gap semiconductors with the valence and conduction bands touching at the Γ point. The calculated Kohn-Sham electronic band structure of the $C222_1$ phases of HgSe and HgTe along two symmetry lines from the Γ point is given in Fig. 15. The band structure of the respective zincblende phases at the same volumes are also given for reference. The transition to $C222_1$ reduces the symmetry and breaks band degeneracies at the Γ point. A small band gap (around 115 meV for HgSe and 150 meV for HgTe in Fig. 15) opens at this point. The maximum of the valence band appears to be also very slightly displaced from Γ along the Γ-L direction by the distortion.

V. CONCLUSIONS

The mercury chalcogenides show peculiar high-pressure behavior within the II–VI family of binary compounds. As an example, HgSe and HgTe exhibit $C222_1$ phases which have not been observed in other binary compounds.[10] In this work we have focused on the stability of the zincblende phases of HgSe and HgTe and the transition to the $C222_1$ structure. These $C222_1$ phases are metastable and are formed only because of the sluggishness of the first-order reconstructive zb→cin transition. We have related the displacive zb→$C222_1$ transition to the softening under pressure of the low-frequency TA(X) modes of the zincblende phase which eventually leads to a dynamical instability and to the $C222_1$ distortion, at pressures not much higher than the observed onset of the zb→cin transition. Indeed, Besson *et al.*[30] observed pretransitional effects in zincblende HgTe under pressure that the authors associated to an overall softening of the phonon branches. It is interesting to note that the higher-pressure NaCl→Cmcm transition observed in HgSe and HgTe as well as in other II–VI and III–V binary compounds[1,9,31] is also related to softening of a TA(X) phonon mode,[32,33] though it has a subtly different nature from the zb→$C222_1$ transition.[13] Full relaxation of the $C222_1$ structure results in a rather small gain in energy in the small range of pressures in which the $C222_1$ phase is observed. The main mechanism for energy gain along the deformation path from zincblende to $C222_1$ in these compounds arises from the internal displacements of the atoms, though the accompanying orthorhombic deformation of the cell (which is mainly due to contraction along the b axis) is structurally important. The $C222_1$ phase appears to be rather soft which may be related to its experimental observation in just a small pressure interval.[10] These results would motivate new experiments on the pressure evolution of the phonon frequencies of the zincblende phases of HgSe and HgTe.

We have tested the stability of the zincblende phase against the $C222_1$ distortion in several other II–VI and III–V compounds.[13] Our results indicate that as pressure increases the zincblende structure eventually becomes unstable against this distortion in other members of these families as well, with a similar mechanism as in the case of HgSe and HgTe [softening of the TA(X) branch of the phonon spectrum].[13] The $C222_1$ distortion can be observed experimentally in HgSe and HgTe simply because this instability occurs at pressures not much higher than the onset of the transition to the high-pressure cinnabar phase. The fact that the frequency of the TA(X) modes is quite small even at zero pressure in zb-HgSe and zb-HgTe obviously has a bearing on this.

ACKNOWLEDGMENTS

S.R. and A.M. acknowledge the financial support of the Ministerio de Educación of Spain through Grants No. MAT2007-65990-C03-03 and No. CSD2007-00045. R.J.N. acknowledges the financial support of the Engineering and Physical Sciences Research Council (U.K.).

[1] R. J. Nelmes and M. I. McMahon, Semicond. Semimetals **54**, 145 (1998).
[2] P. W. Bridgman, Proc. Am. Acad. Arts Sci. **74**, 21 (1940).
[3] N. G. Wright, M. I. McMahon, R. J. Nelmes, and A. San-Miguel, Phys. Rev. B **48**, 13111 (1993).
[4] A. San-Miguel, N. G. Wright, M. I. McMahon, and R. J. Nelmes, Phys. Rev. B **51**, 8731 (1995).
[5] T.-L. Huang and A. L. Ruoff, Phys. Rev. B **31**, 5976 (1985).
[6] T.-L. Huang and A. L. Ruoff, Phys. Rev. B **27**, 7811 (1983).
[7] M. I. McMahon, N. G. Wright, D. R. Allan, and R. J. Nelmes, Phys. Rev. B **53**, 2163 (1996).
[8] R. J. Nelmes, M. I. McMahon, N. G. Wright, and D. R. Allan, Phys. Rev. Lett. **73**, 1805 (1994).
[9] A. Mujica, A. Rubio, A. Muñoz, and R. J. Needs, Rev. Mod. Phys. **75**, 863 (2003).
[10] M. I. McMahon, R. J. Nelmes, H. Liu, and S. A. Belmonte, Phys. Rev. Lett. **77**, 1781 (1996).
[11] Z. W. Lu, D. Singh, and H. Krakauer, Phys. Rev. B **39**, 10154 (1989).
[12] S.-R. Sun and Y.-H. Dong, Phys. Rev. B **72**, 174101 (2005).
[13] S. Radescu *et al.* (unpublished).
[14] G. Kresse and J. Furthmüller, Comput. Mater. Sci. **6**, 15 (1996); Phys. Rev. B **54**, 11169 (1996). For more information see: http://cms.mpi.univie.ac.at/vasp
[15] G. Kresse and D. Joubert, Phys. Rev. B **59**, 1758 (1999).
[16] D. M. Ceperley and B. J. Alder, Phys. Rev. Lett. **45**, 566 (1980); as parametrized by J. P. Perdew and A. Zunger, Phys. Rev. B **23**, 5048 (1981).
[17] J. P. Perdew, K. Burke, and M. Ernzerhof, Phys. Rev. Lett. **77**, 3865 (1996).
[18] R. W. G. Wyckoff, *Crystal Structures* (Interscience, New York, 1963).
[19] H. D. Megaw, *Crystal Structures: A Working Approach* (W. B. Saunders, Philadelphia, London, Toronto, 1973).
[20] *Data in Science and Technology: Semiconductors other than Group IV elements and III-V compounds*, edited by O. Madelung (Springer-Verlag, Berlin, 1992), and references therein.
[21] K. Aurivillius and I.-B. Carlsson, Acta Chem. Scand. (1947-1973) **11**, 1069 (1957); **12**, 1297 (1958).
[22] S. B. Qadri, A. W. Webb, E. F. Skelton, N. Moulton, J. Furdyna, and L. Colombo, High Press. Res. **4**, 303 (1990).
[23] Such a pattern of distortion reduces the cubic $F\bar{4}3m$ symmetry of the zincblende structure to the orthorhombic $C222_1$ symmetry, and thus the displacement of atoms at the transition is accompanied by an orthorhombic deformation of the cell.
[24] D. Alfè, G. D. Price, and M. J. Gillan, Phys. Rev. B **64**, 045123 (2001). Program available at http://chianti.geol.ucl.ac.uk/dario
[25] G. Kresse, J. Furthmüller, and J. Hafner, Europhys. Lett. **32**, 729 (1995).
[26] The supercell method does not however give correct values of the LO-TO splitting which occurs near the Γ point. The details of the phonon band structure near the zone center are nonetheless irrelevant in the present stability study, which is mainly concerned with the zone-boundary X point.
[27] It also has extremal variation, that is, a maximum in the absolute value of its Grüneisen parameter.
[28] Following normal practice, the negative frequencies in these plots correspond to the negative value of the modulus of the (complex) eigenvalues of the dynamical matrix.
[29] The direction of *maximum* energy variation corresponds in turn to the eigenvector of the TO "hard" mode at X.
[30] J. M. Besson, P. Grima, M. Gauthier, J. P. Itié, M. Mézouar, D. Häusermann, and M. Hanfland, Phys. Stat. Solidi B **198**, 419 (1996).
[31] A. Mujica, R. J. Needs, and A. Muñoz, Phys. Rev. B **52**, 8881 (1995).
[32] V. Ozoliņš and A. Zunger, Phys. Rev. Lett. **82**, 767 (1999).
[33] A. Mujica and R. J. Needs, J. Phys.: Condens. Matter **8**, L237 (1996).